NEOPLASIA
www.neoplasia.com

Volume 16 Number 8 August 2014 pp. 665–677 665

Antitumor Action of a Novel Histone Deacetylase Inhibitor, YF479, in Breast Cancer[1]

Tao Zhang*, Yihua Chen*, Jingjie Li*, Feifei Yang*, Haigang Wu*, Fujun Dai*, Meichun Hu*, Xiaoling Lu‡, Yi Peng‡, Mingyao Liu*,†, Yongxiang Zhao‡ and Zhengfang Yi*

*Shanghai Key Laboratory of Regulatory Biology, Institute of Biomedical Sciences and School of Life Sciences, East China Normal University, 500 Dongchuan Road, Shanghai 200241, China; †Center for Cancer and Stem Cell Biology, Institute of Biosciences and Technology, Texas A&M University Health Science Center, Houston, TX 77030; ‡Biological Targeting Diagnosis and Therapy Research Center, Guangxi Medical University, 22 Shuang Yong Rd. Nanning, Guangxi 530021, China

Abstract

Accumulating evidence demonstrates important roles for histone deacetylase in tumorigenesis (HDACs), highlighting them as attractive targets for antitumor drug development. Histone deactylase inhibitors (HDACIs), which have shown favorable anti-tumor activity with low toxicity in clinical investigations, are a promising class of anticancer therapeutics. Here, we screened our compound library to explore small molecules that possess anti-HDAC activity and identified a novel HDACI, YF479. Suberoylanilide hydroxamic acid (SAHA), which was the first approved HDAC inhibitor for clinical treatment by the FDA, was as positive control in our experiments. We further demonstrated YF479 abated cell viability, suppressed colony formation and tumor cell motility *in vitro*. To investigate YF479 with superior pharmacodynamic properties, we developed spontaneous and experimental breast cancer animal models. Our results showed YF479 significantly inhibited breast tumor growth and metastasis *in vivo*. Further study indicated YF479 suppressed both early and end stages of metastatic progression. Subsequent adjuvant chemotherapy animal experiment revealed the elimination of local-regional recurrence (LRR) and distant metastasis by YF479. More important, YF479 remarkably prolonged the survival of tumor-bearing mice. Intriguingly, YF479 displayed more potent anti-tumor activity *in vitro* and *in vivo* compared with SAHA. Together, our results suggest that YF479, a novel HDACI, inhibits breast tumor growth, metastasis and recurrence. In light of these results, YF479 may be an effective therapeutic option in clinical trials for patients burdened by breast cancer.

Neoplasia (2014) 16, 665–677

Abbreviations: HDAC, histone deacetylase; HDACIs, Histone deacetylase inhibitors; SAHA, Suberoylanilide hydroxamic acid; LRR, local-regional recurrence; HATs, Histone acetyltransferases; VPA, Valproic acid; DAPI, 4, 6-diamidino-2-phenylindole; PCNA, proliferation cell nuclear antigen; PARP, Poly ADP ribose polymerase; MMP, Matrix metalloproteinase; TIMP, Tissue inhibitor of MMP

Address all correspondence to: Drs. Zhengfang Yi or Yongxiang Zhao or Mingyao Liu, Institute of Biomedical Sciences, East China Normal University, 500 Dongchuan Road, Shanghai 200241, China.
E-mail: zfyi@bio.ecnu.edu.cn or yongxiangzhao@126.com or mliu@ibt.tamhsc.edu

[1]Funding: This work was supported in parts by Major State Basic Research Development Program of China (2012CB910400, 2009CB918402). National Natural Science Foundation of China (30930055, 30971523, 81071807, 81272463 and 81172139). Program for Changjiang Scholars and Innovative Research Team in University (IRT1119 and IRT1128). Innovation Program of Shanghai Municipal Education Commission (13zz034). The Science and Technology Commission of Shanghai Municipality (11DZ2260300,12XD1406100). Research Fund for the Doctoral Program of Higher Education of China (20120076120029).
Received 22 May 2014; Revised 23 July 2014; Accepted 29 July 2014

1476-5586/14
http://dx.doi.org/10.1016/j.neo.2014.07.009

Introduction

Cancer has conventionally been considered as a disease involving genetic defects that result in oncogene activation or loss of tumor suppressor genes [1]. However, epigenetic changes including histone acetylation, also contribute to tumor development [2]. Histone acetyltransferases and deacetylases (HDACs) play a central role in chromatin structure modification and gene expression [3,4]. Histone acetyltransferase inactivation is associated with tumorigenesis [5]. Aberrant HDAC activity is proposed to be the key event in tumor formation, since excessive HDAC activity inappropriately repressed transcription of tumor suppressor genes [6].

Recently, more and more evidence has shown that HDAC inhibitors induced tumor cell differentiation, apoptosis, and/or growth arrest in several cell culture and tumor xenograft models. Based on the chemical structure, HDACIs can be categorized into four main different classes, including short-chain fatty acids, hydroxamates, benzamides and cyclic tetrapeptides. The short-chain fatty acid sodium butyrate and the hydroxamic acid trichostatin A were found relatively early to be HDAC inhibitors, but both have limits to their clinical activity [7]. The trichostatin A structural analog Suberoylanilide hydroxamic acid (SAHA) has shown promise in cancer therapy. It was the first approved HDAC inhibitor for clinical treatment by the FDA [8]. Other compounds from structurally different families, such as LBH589, valproic acid, MS-275 and FK-228 have been used in pre- and clinical trials [9]. In addition, several active trials of HDACI combined with other antitumor agents are ongoing in patients with solid and hematological malignancies [10].

Breast cancer is the most common cancer diagnosed in women and the second leading cause of cancer-related death worldwide [11]. Despite significant advances in the diagnosis and treatment of breast cancer, many patients succumb to this disease. In recent years, accumulating research strongly supports HDACs as molecular targets for anticancer therapy in breast cancer [12,13]. Several HDACIs are being evaluated as single agents or combined with conventional therapies in clinical trials of metastatic breast cancer [12,14,15]. Based on these backgrounds, it is necessary to develop novel HDAC inhibitors for breast cancer therapeutics.

In this study, we identified a novel HDACI, YF479, which displays potent anti-breast tumor activity. *In vitro*, YF479 inhibited cell growth, induced apoptosis and G2/M cell cycle arrest, and suppressed cell motility. We further demonstrated the inhibitory efficacy of YF479 in breast cancer growth, metastasis and recurrence using preclinical animal models. Interestingly, YF479 showed stronger anti-tumor activity *in vitro* and *in vivo* compared to SAHA. In conclusion, these findings provide the proof-of-concept for evaluation of YF479 as a breast cancer therapeutic agent.

Materials and Methods

Cell Culture, Animals, and Reagents

Breast tumor cell lines MDA-MB231, 4 T1 and T47D were obtained from American Type Culture Collection. All these cells were maintained in American Type Culture Collection recommended cell culture media and conditions. MDA-MB231-luc (which stably expresses the luciferase reporter gene and can be tracked by bioluminescence) was cultured in MEM medium supplemented to 10% fetal bovine serum and nonessential amino acids [16]. 4 T1-luc was cultured in DMEM medium supplemented to 10% fetal bovine serum [17].

All animals were purchased from the National Rodent Laboratory Animal Resources, Shanghai Branch of China. The mice were housed and maintained in the animal vivarium of East China Normal University and all of the experimental protocols were approved by the Animal Investigation Committee of the Institute of Biomedical Sciences and School of Life Sciences, East China Normal University.

YF479 were synthesized as described in the Supplementary Information. SAHA was described previously [18]. Compound stock solutions were prepared in dimethyl sulfoxide (DMSO) at a concentration of 50 mM and stored at −20°C. Matrigel was purchased from BD biosciences. All antibodies were purchased from Cell Signaling Technology, except anti-p21 (Santa Cruz) and anti-actin (Sigma).

HDAC Activity Assay

HDAC activity was determined using the colorimetric HDAC activity assay kit (BioVision, Inc.) according to the manufacturer's instruction. Briefly, HDAC enzymes (Hela nuclear extract or MDA-MB231 cell lysate) were incubated with SAHA or test compounds in the presence of HDAC substrate (Boc-Lys (Ac)-AMC) at 37°C for 1 hour. Then the lysine developer was added to terminate the reaction, and the samples were incubated at 37°C for another 30 minutes. The fluorescence intensities were determined in a fluorometer (FLUOstar OPTIMA, BMG LABTECH) with excitation at 355 nm and emission at 460 nm. Three independent experiments with triplicate were carried out.

Western Blot Analysis

MDA-MB231, 4 T1 or T47D were treated with YF479 or SAHA for indicated time; then cells were lysed in RIPA buffer. Primary tumors were well minced, and lysed with RIPA buffer. Protein concentration was determined using a Bicinchoninic acid assay (Thermo Scientific). Whole samples were run on 8% to 12% SDS-PAGE gels and transferred to polyvinylidene difluoride membranes (Gibco). The membranes were incubated overnight using specific antibodies. The visual signals were visualized by chemiluminscence western blotting reagent (ECL kit) and autoradiograph film.

Immunofluorescence Saining Assay

For immunofluorescence staining of tumor cells, human breast tumor cells were plated onto gelatin-coated coverslips. After treatment with or without compounds (as indicated in the figure) for 24 hours, cells were fixed with 3.7% paraformaldehyde for 15 minutes at room temperature, permeabilized with 0.1% Triton X-100 for 5 minutes, and then blocked with 1% BSA for 1 hour. Cells were incubated with specific primary antibody (as indicated in the figures) overnight. After washing with PBS, cells were incubated with the appropriate secondary antibody for 1 hour. Phalloidin and 4,6-diamidino-2-phenylindole were further used to stain F-actin and nucleus, respectively. Photographs were obtained with a Leica Confocal microscope.

MTS Assay

MDA-MB231, 4 T1 and T47D (5×10^3 cells/well) were treated with various concentrations of YF479 for 48 hours. To detect cell viability, the Aqueous one Solution (Promega) was used according to manufacturer instructions, and the absorption of 490 nm was measured.

Cell Cycle Analysis

Cell cycle analysis was conducted as described [19]. Briefly, MDA-MB231 cells were treated with YF479 or SAHA for 24 hours followed by PBS washes. Cells were then fixed with cold 70% ethanol at 4 °C for at least 12 hours. PI working solution was added before flow cytometry analysis (FACS Calibur, BDbiosciences).

Apoptosis Assay

Apoptosis was measured using the Apoptosis Detection Kit (BD Biosciences) as described [20]. Briefly, MDA-MB231, 4 T1 and T47D cells were treated with YF479 or SAHA for 48 hours. Then cells were collected, washed, and stained with annexin V–FITC and PI for 15 minutes before evaluation by flow cytometry (FACS Calibur, BDbiosciences).

Tumor Cell Clonogenic Assay

To mimic individual cell development into macroscopic cell clones, the cell clonogenic assay was performed as previously described [21]. Tumor cells were seeded into 6-well plate and allowed to grow for 24 hours. Cells were then treated with different concentrations of YF479 or SAHA. On day 8, colonies were fixed in 3.7% paraformaldehyde, stained with 0.1% crystal violet and counted manually.

Adhesion Assay

Adhesion assay was performed as previously reported [22] with modifications. In brief, tumor cells were pretreated with DMSO or different concentrations of YF479 for 12 hours, and then trypsinized. Cells (1×10^5/well) were added into 96-well plates with or without YF479 for 25 minutes at 37 °C. Non-adherent cells were removed by a gentle wash with PBS and the remaining cells were stained with 0.1% crystal violet for 5 minutes. After extensive washing, the precipitates were dissolved by addition of 30% acetic acid, and the absorption was obtained at 590 nm. The percentage of inhibition was expressed using control well as 100%.

Migration Assay

The inhibition of tumor cell migration by YF479 or SAHA was determined by wound-healing migration assay [23]. Briefly, tumor cells were allowed to grow into full confluence in 6-well plates, and then the "wounds" were created by a sterile pipette tip. Fresh medium containing 10% fetal bovine serum and various concentrations of YF479 or SAHA was added. After 12 hours incubation at 37 °C, cells were fixed with 3.7% paraformaldehyde and photographed. The migrated cells were manually quantified. The percentage inhibition of migrated cells was expressed using the untreated group as 100%.

Invasion Assay

Invasion assay was performed using transwell chambers (Corning) with 8 μm pore membranes coated with Matrigel as described previously [24]. In brief, after 12 hours pretreatment with YF479 or SAHA in 6-well plate, tumor cells were detached with trypsin and resuspended as signal cells. A total of 5×10^4 cells (for MDA-MB231) or 10×10^4 cells (for 4 T1) in 100 μL of serum-free medium were added in the upper chamber, and 600 μL of complete medium was added at the bottom. Different concentrations of YF479 or SAHA were added to both chambers. The cells were allowed to invade for 9–12 hours at 37 °C. Invaded cells were stained with 0.1% crystal violet and counted manually. The percentage of inhibition was expressed using control well as 100%.

Gelatin zymography assay

Gelatin zymography was performed as previously described [25]. Conditional media were collected after the cells were plated at equal densities in 10 cm dishes and then serum starved in 5 ml of basal media containing different concentrations of YF479 for 24 hours. The conditional media were concentrated and equal amount of samples were mixed with sample buffer and applied to 8% SDS-polyacrylamide gel copolymerized with 1 mg/mL of gelatin. After running, the gel was incubated in renaturing buffer (2.5% Triton X-100, 50 mM Tris-base, 200 mM NaCl, 10 mM $CaCl_2$ and 1 μM $ZnCl_2$,) followed by a 24 hours incubation with developing buffer (50 mM Tris-base, 200 mM NaCl, 10 mM $CaCl_2$ and 1 μM $ZnCl_2$, 0.2% Brij35). The gel was then stained with 0.25% coomassie blue R-250 for 1 hour and destained with coomassie blue destaininig water. Clear bands against the dark blue background where the protease has digested the gelatin indicated protease activity.

MDA-MB231 Xenograft Animal Model

MDA-MB231-luc cells (1×10^6 in 0.1 mL PBS) were inoculated into the mammary fat pads of nude mice. On day 5, we used an Xenogen IVIS 2000 Luminal Imager (IVIS imaging system 100, Xenogen Corporation) to make sure the same number of tumor cells were inoculated in each mouse, and then divided the mice into 4 groups (n = 6 per group). Thereafter, the mice received an i.p. injection with YF479 (20 mg/kg or 30 mg/kg), SAHA (30 mg/kg) or DMSO every day. The change of primary tumor size was monitored by IVIS Imaging System. On day 30, mice were euthanized by cervical dislocation under isoflurane anesthesia. Half of each primary tumor was snap frozen in liquid nitrogen for western blotting. The other half were fixed and prepared for immunohistochemical analyses. The excised lungs were individually scanned for the presence of bioluminescent metastatic cells.

Experimental Metastasis Animal Model

MDA-MB231-luc cells (1×10^6 in 0.1 mL PBS) were injected into the lateral tail vein of female nude mice. The mice were then segregated into 4 groups (n = 7 per group) based on initial IVIS image. Starting from day 0, mice were administered with YF479 (20 mg/kg or 30 mg/kg), SAHA (30 mg/kg) or DMSO every day. On day 30, after the last IVIS detection, mice were euthanized and lung tissues were removed from each mouse for immunohistochemical analyses.

Immunohistochemistry Analyses

Immunohistochemistry was performed as previously reported [21]. Primary tumors and lungs were excised, fixed and embedded in paraffin. To investigate the effect of YF479 on tumor cells proliferation and apoptosis in vivo, sections (4 μm) were stained with anti-proliferation cell nuclear antigen (PCNA) and cleaved caspase-3. Images were obtained with Leica microscope (Leica, DM4000b). The results were analyzed using Image-Pro Plus 6.0 software.

Early and Advanced Metastasis Stage Animal Model

This animal experiment was performed as previously described [26]. MDA-MB231-luc cells (1×10^6 in 0.1 mL PBS) were injected into the lateral tail vein of female nude mice which were subsequently divided into 4 groups (n = 7 per group) according to the initial bioluminescence. Two groups received early-stage treatment and were injected intraperitoneally with YF479 (30 mg kg^{-1} day^{-1}) or DMSO from day 0 to day 7 and the other two groups received late-stage treatment, injections from day 7 to day 15. On day 28, tumor cells in mice were detected by Xenogen IVIS 2000 Luminal Imager.

Adjuvant therapy animal model

Adjuvant therapy animal experiment was performed as previously described [27]. Mouse breast tumor cells 4 T1-luc

(1×10^5 in 0.1 mL) were inoculated into the fourth mammary fat-pad of female BALB/c mice. On day 8, mice were assigned into four groups (n = 11 per group) and anesthetized, to surgically removed the primary tumor; the wound was closed with surgical clips. From day 9, YF479 (20 mg/kg or 30 mg/kg), SAHA (30 mg/kg) or DMSO were administered every day by intraperitoneal injection. Tumor recurrence and distant metastasis in mice was monitored using *in vivo* bioluminescence imaging on day 30.

Statistical Analysis

Unless otherwise noted, statistical analyses were performed using the Student's t-test. All experiments were repeated at least three times except animal experiments. $P < .05$ was considered significant.

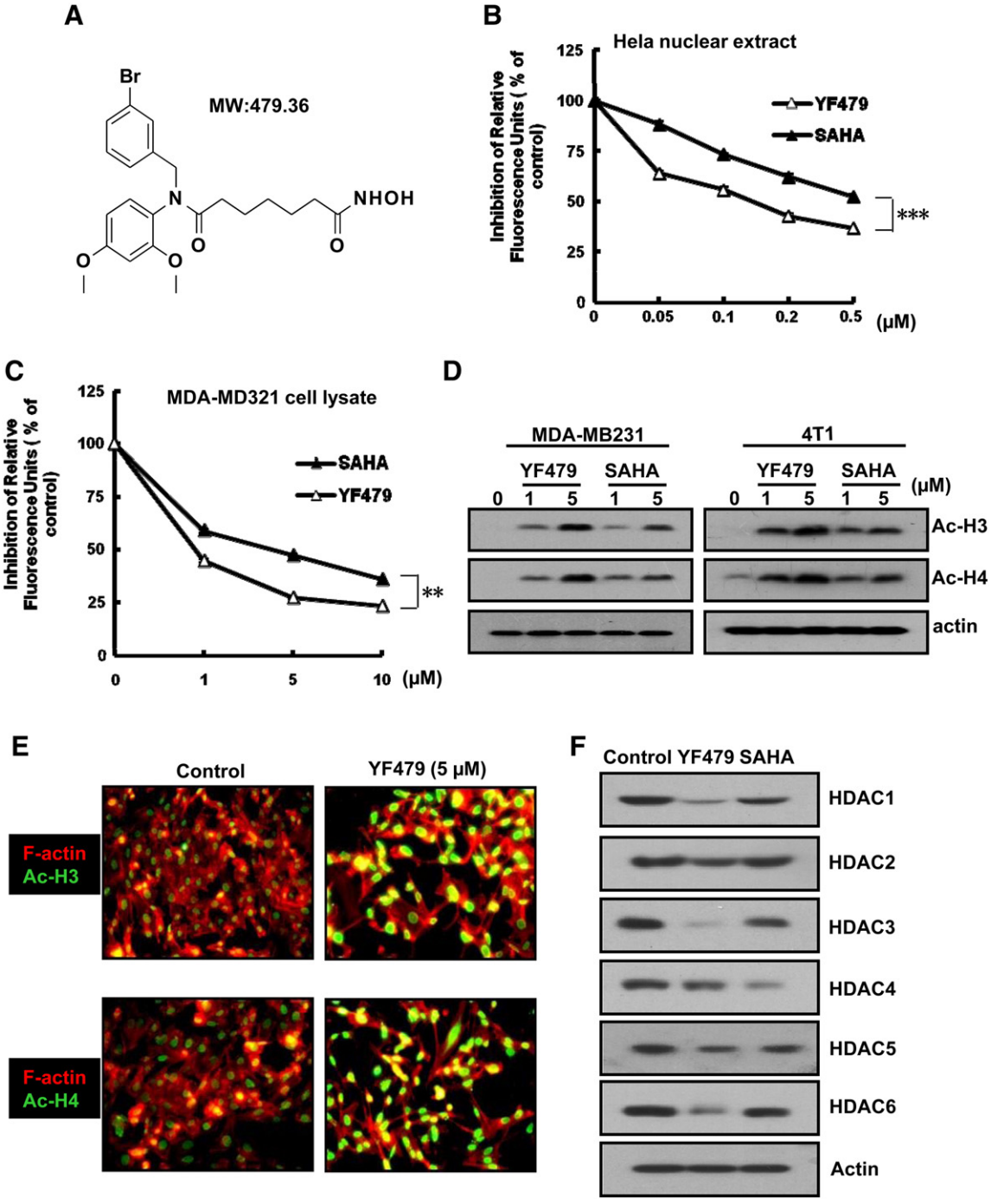

Figure 1. YF479 is a bona fide HDAC inhibitor. (A) Chemical structure of the HDACi, YF479. (B) and (C) Hela nuclear extract or MDA-MB231 lysates were treated with different dosages of YF479 or SAHA for 1 hour, and HDAC activity was measured. (D) MDA-MB231 or 4 T1 cells were treated with YF479 or SAHA (at indicated concentration) for 24 hour. Western blotting was performed for analyzing the acetylated histone H3,4 (Ac-H3, Ac-H4) levels. (E) MDA-MB231 cells were seeded on gelatin-coated coverslips. Cells were then treated with YF479 for 24 hour, fixed, and stained with the indicated antibodies. (F) MDA-MB231 cells were treated with YF479 (10 μM) or SAHA (10 μM) for 24 hours. Western blotting was performed to analyze the expression of HDACs in MDA-MB231 cells treated with YF479 or SAHA. All experiments were repeated at least three times. $^{**}P < .01$; $^{***}P < .001$.

Results

YF479 Is a Bona Fide HDAC Inhibitor

Using a HDACs inhibiton assay screen, we identified a novel small molecule YF479 (N1-(3-bromobenzyl)-N7-hydroxy- N1-(2,4-dimethoxyphenyl) heptanediamid; MW: 479.36) with the highest HDAC inhibitory activity in our internal chemical library (about 150 compounds). The chemical structure was showed in Figure 1*A*. Further synthesis experimental details and purity analysis are specified in Supplementary Figure S1 and supplementary method. We tested the histone deacetylase inhibitory activity of YF479 vis-a-vis that of SAHA in detail. The results indicated YF479 and SAHA inhibited HDAC activity in a dose-dependent manner (Figure 1, *B* and *C*) and the inhibitory efficacy of YF479 was stronger than that of SAHA. A hallmark index of HDAC inhibition *in vivo* is the acetylation of histones H3 and H4 [28]. We therefore tested the effect of YF479 and SAHA on the acetylation level of H3 and H4 via western blot and cell immunofluorescence staining assay. As shown in Figure 1, *D* and *E*, either YF479 or SAHA significantly upregulated acetylated H3 and H4. In addition, our data demonstrated that YF479 down-regulated the expression of HDAC 1, 2, 3, 4, 5 and 6 (Figure 1*F*). These initial results suggested that YF479 is a bona fide HDACI, supporting further examination of YF479 in breast cancer treatment *in vitro* and *in vivo*.

YF479 Soaks into HDACs in Docking Model

To explore how YF479 interacted with HDACs, molecular docking models of YF479 with x-ray crystal structure of HDACs (HDAC1 (PDB ID: 4BKX); HDAC2 (PDB ID: 3MAX) and HDAC3 (PDB ID: 4A69) were carried out by the autodock 4.2 and UCSF Chimera 1.7. The results from our predictive models showed that YF479 could bind to the active domains of HDACs (Supplementary Figure S4). For example, a hydrogen bond was observed to form by the N-H group of imidazole of protonated His178 in HDAC1 with carbonyl group of YF479 which was near the two aromatic groups (Supplementary Figure S4*a*1). Through hydrophobic interaction, 3-bromophenyl and 2, 4-dimethoxylphenyl in YF479 were approached the hydrophobic area which was formed by Pro 29, Phe 150, Phe 205, Leu 271 and Tyr 303 residues. The alkyl liner could insert the pocket and interacted with Phe 150 and Phe 205 residues (Supplementary Figure S4*a*2). The hydroxamic group interacted with the zinc ion to form the coordinate bond (Supplementary Figure S4*A*). For the HDAC2 (Supplementary Figure S4*B*), a similar hydrogen bond was also observed to form by His183 in HDAC2 with carbonyl group of YF479 which was near the two aromatic groups (Supplementary Figure S4*b*1). Two phenyl groups in YF479 interacted with the Pro34, Phe155, Tyr209, Leu276 and Tyr308 of active site through hydrophobic interaction. The inhibitor with alkyl linker could insert into the pocket and interact with the hydrophobic area which was formed by Phe155 and Phe210 in this pocket (Supplementary Figure S4*b*2). At last, the hydroxamic group interacted with the zinc ion to form the coordinate bond. We also found that the interactions of YF479 with HDAC3 were similar to that with HDAC1 or HDAC2 through analysis of docking models (Supplementary Figure S4*C*). From all the docking data of YF479 with HDACs, we thought that YF479 could bind to HDACs with good interactions.

YF479 Retards Breast Cancer Cell Growth in Vitro

Tumor cells sustain limitless growth by continually proliferating and evading apoptosis [29]. To determine the effect of YF479 on breast cancer cell growth, we performed the MTS proliferation assay. As shown in Figure 2*A*, YF479 inhibited cell proliferation in a dose-dependent manner in three different breast cancer cell lines, and the IC50 ranged from 1 to 2.5 μM. Then, we evaluated whether the anti-growth activity of YF479 was due to effects on cell cycle progression and/or apoptosis. Our results showed that YF479 induced cell-cycle arrest at the G2/M phase in MDA-MB231 cells and FACS analysis showed increased cellular accumulation in the sub-G1 cell cycle fraction, suggesting drug-induced tumor cell proliferation and apoptosis (Figure 2*B*) [30,31]. Furthermore, YF479 caused a dose-dependent induction of apoptosis as determined by Annexin V staining (Figure 2*C*). We also studied the effect of YF479 on colony formation, since colony formation of tumor cells is closer to its physiology and growth *in vivo*. Results showed that YF479 (1 μM) significantly inhibited MDA-MB231 and 4 T1 cells colony formation (Figure 2*D*). Additionally, We performed western blotting assay to detected the expression level of tumor cell proliferation (PCNA), cell cycle (p21,cdc2 and cyclinB1) and apoptosis related proteins (PARP, cleaved-PARP, caspase 3, and cleaved-caspase 3) after YF479 treatment [32–35]. The result showed YF479 down-regulated the expression of PCNA, cdc2, cyclinB1, PARP and caspase 3, while upregulated p21, cleaved-caspase 3 and cleaved-PARP expression. SAHA was used as the positive control in all the above assays (Figure 2*E* and Supplementary Figure S5). These experiments suggested that YF479 suppressed breast cancer cell growth, further supporting the testing of *in vivo* efficacy of YF479 in breast cancer.

YF479 Shows Potent Metastasis-Inhibitory Effects on Human and Murine Breast Cancer Cells

Tumor cell escape from the primary tumor to metastatic sites is a multistep process, which requires loss of cell adhesion, and acquisition of migration and invasion capability. To determine the effect of YF479 treatment on breast cancer metastasis, we performed cell adhesion, migration, and invasion assays using highly malignant murine breast cancer cell 4 T1 and human breast cancer cell MDA-MB231. YF479, in a dose-dependent manner, significantly inhibited tumor cell adhesion (Figure 3*A* panel *a*1), migration (Figure 3*A* panel *a*2), and invasion (Figure 3*A* panel *a*3 and Figure 3*B*) in both 4 T1 and MDA-MB231 breast cancer cells. In order to investigate whether the reduced cell adhesion, and motility by YF479 were due to its growth suppression activity, we performed MTS assay. Little growth inhibitory effect of YF479 was observed within the same time frame as the cell adhesion and motility assay (data not shown). Increasing evidence shows the importance of paxillin in breast cancer morphology, invasion and metastasis [36–38], and the paxillin signaling axis may represent a potential therapeutic target and/or prognostic marker in breast cancer metastasis [39]. To preliminarily explore the mechanism of YF479 on anti-metastasis, we detected the expression of paxillin and the spindle microtubule protein acetylated alpha-tubulin (Ac-tubulin), the marker of primary cilia, which participates in the development and progression of cancer, including breast cancer [40]. Results showed that YF479 significantly upregulated Ac-tubulin expression and markedly down-regulated the expression of paxillin (Figure 3*C*). Matrix metalloproteinases (MMPs) play critical roles in cancer-cell invasion and metastasis and numerous studies revealed inhibition of MMPs via synthetic and natural inhibitor (TIMP: Tissue inhibitor of MMP) suppress tumor cell invasion [41]. The result showed YF479 down-regulated the expression level of MMPs (MMP2 and MMP9) and upregulated TIMPs (TIMP1 and TIMP2) expression (Supplementary Figure S6*A*). Furthermore, we found YF479 inhibited MMPs activity

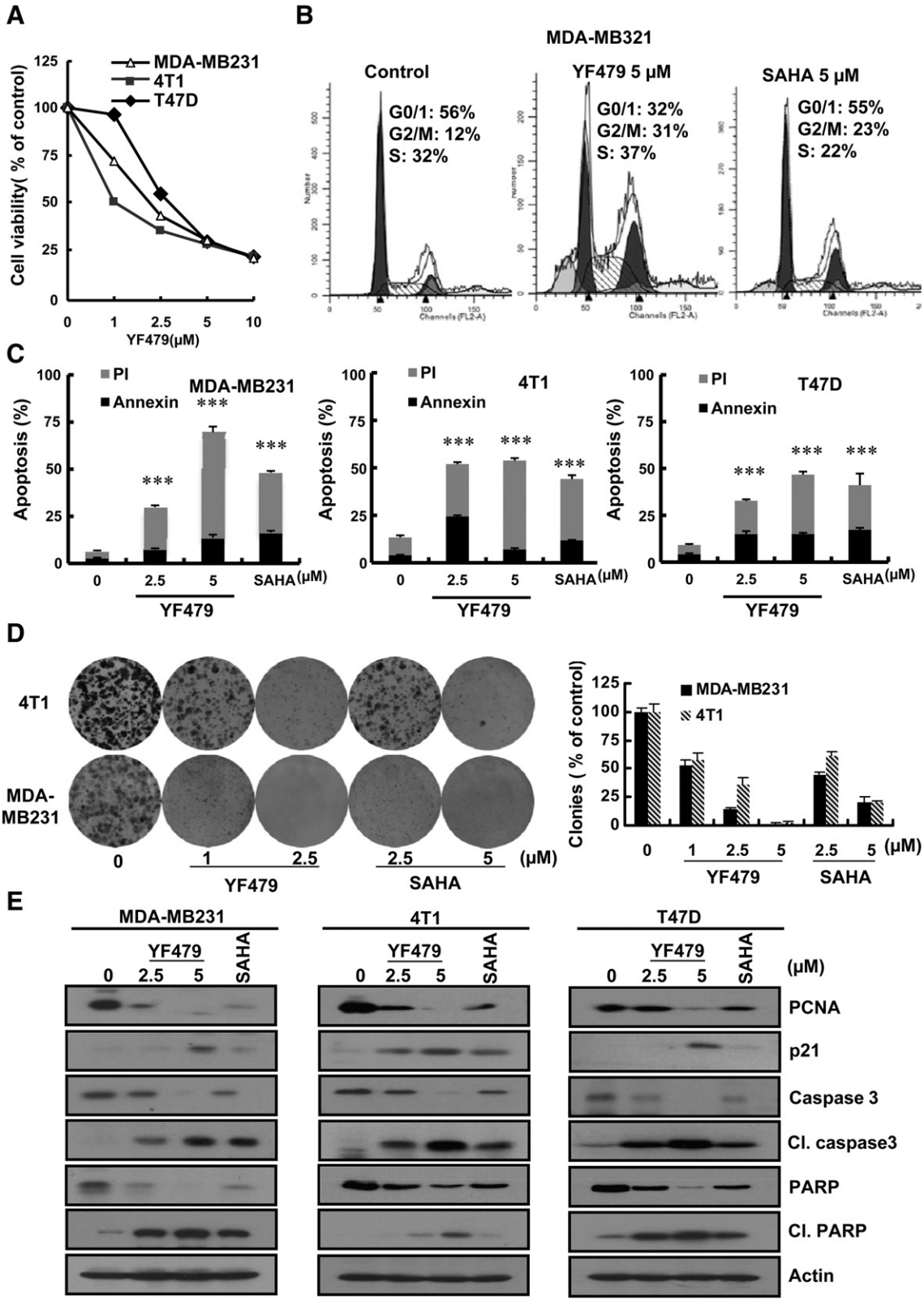

Figure 2. YF479 inhibits breast tumor cell growth *in vitro*. (A) MDA-MB231, 4 T1 and T47D cells were treated with indicated concentrations of YF479 for 48 hours. Cell viability was assessed by MTS assay (n = 3). (B) MDA-MB231, 4 T1 and T47D cells were treated with 5 μM YF479 or 5 μM SAHA for 24 hours. Cell cycle distribution was then evaluated using propidium iodide (PI) staining and flow cytometry (n = 3). (C) MDA-MB231, 4 T1 and T47D cells were treated with indicated concentrations of YF479 and 5 μM SAHA for 48 hours. Apoptosis was assessed by Annexin V/PI staining and flow cytometry (n = 3). (D) YF479 and SAHA abrogate cancer cell colony formation capacity (8 days). Number of colonies counted in experiments repeated three times. Results represent the average of three replications. (E) MDA-MB231, 4 T1 or T47D cells were incubated with various concentrations of YF479 and 5 μM SAHA for 48 hours. Effects on the expression of PCNA, p21, caspase 3, cleaved –caspase 3, PARP and cleaved-PARP were determined by western blot. Actin was used as a loading control. $^{**}P < .01$; $^{***}P < .001$.

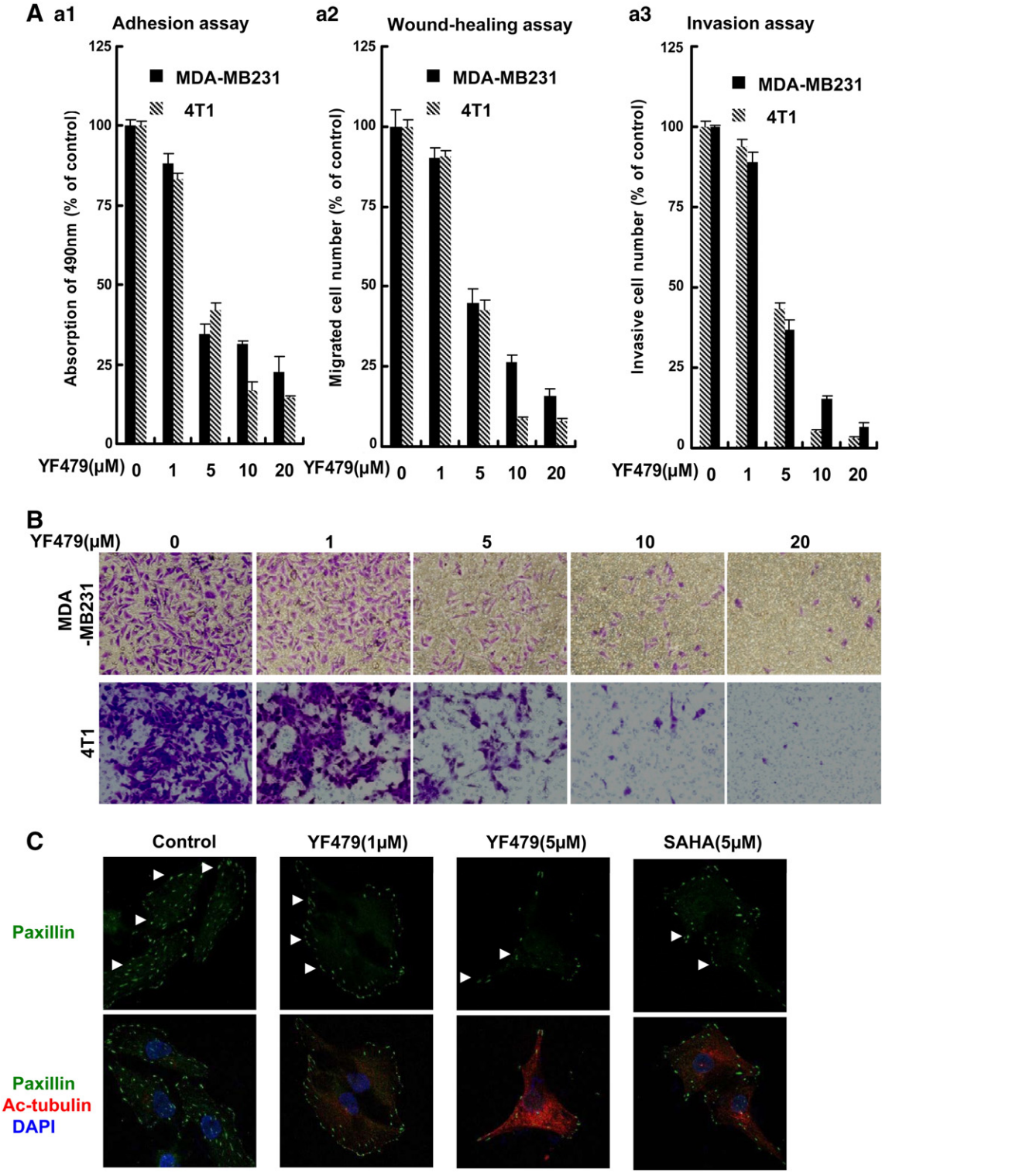

Figure 3. YF479 inhibits breast cancer cell adhesion, migration and invasion. (A) YF479 suppresses MDA-MB231 and 4 T1 breast cancer cell adhesion, migration and invasion. a1, Adhesion assay. Tumor cells were pretreated with various concentrations of YF479 for 12 hours; Cells were trypsinized, and seeded on a fibronectin coated 96-well plate. After 25 minutes, non-adherent cells were removed and adherent cells were stained with 0.1% crystal violet. The precipitates were dissolved in 30% acetic acid, and the absorption at 590 nm was acquired. a2, Wound-healing migration assay. Tumor cells were seeded in six-well plates. A "wound" was created after the cells grew into full confluence, then different concentrations YF479 and SAHA were added. After incubation for 12 hours, all the groups were fixed and photographed. a3, YF479 inhibits MDA-MB231 and 4 T1 invasion. Tumor cells were treated with different concentrations of YF479 and allowed to invade through Matrigel. Invaded cell number was counted. (B) Representative images of a3. (C) MDA-MB231 cells were treated with YF479 for 24 hours. The immunofluorescence assay showed the expression level of paxillin and Ac-tubulin. All experiments were repeated at least three times.

by gelatin zymography assay (Supplementary Figure S6*B*). Previous study reported that SAHA limited tumor cell migration and invasion [42], our results were in accordance with these studies (Supplementary Figure S7). The above results suggested that YF479 showed metastasis-inhibitory effects on human and murine breast cancer cells.

YF479 Inhibits Tumor Growth and Metastasis in a Mouse Orthotopic Implantation Model

Having shown the anti-tumor effects of YF479 *in vitro*, we next determined whether these *in vitro* effects correlate with the *in vivo* activity of YF479 using a mouse model. MDA-MB231-luc cells were injected into the mammary fat pad of nude mice. Using whole-body bioluminescence imaging, we monitored primary growth development over 30 days. During 30 days, the rate of tumor growth decreased in mice treated with YF479 (20 mg/kg and 30 mg/kg) or SAHA (30 mg/kg), as compared with mice injected with DMSO (Figure 4*A*). We found a significant different growth rate between control and treated groups (30 mg/kg YF479) ($p < 0.01$) (Figure 4*B*). All mice were sacrificed on day 30, and excised lungs were individually scanned for the metastatic cells. Results of statistical analysis showed a lower incidence of lung metastasis in YF479-treatment groups than that in the control group. Notably, the incidence of lung metastasis in the YF479-treated mice (30 mg/kg) was lower than that in the SAHA-treatment group under the same dosage (Figure 4*C*).

To better understand the mechanism by which YF479 suppressed primary tumor growth, we analyzed tumor histone acetylation, proliferation and apoptosis. The increased Ac-H3 and Ac-H4 levels in primary tumor tissue of YF479 treated mice confirmed the HDAC inhibitory effect of YF479 on breast cancer (Figure 4*D*). In addition, results showed that YF479 more strongly increased Ac-H3 and Ac-H4 levels. These results suggested that YF479 could effectively inhibit HDAC activity *in vivo*. Histological analysis showed that the expression of PCNA was decreased and cleaved-caspase 3 levels were increased and the sensitivity of tumor apoptosis in the YF479-treated group was higher than that in SAHA treated mice (Figure 4*E*), which was in consistent with our results *in vitro* (Figure 2*C*).

YF479 Inhibits Breast Tumor Metastasis to the Lungs in an Experimental Metastasis Animal Model

We have shown that YF479 inhibited breast cancer cell adhesion, migration and invasion *in vitro*. Next, we tested the efficacy of YF479 in attenuating the metastatic propensity of breast carcinoma cells using an *in vivo* model of experimental metastasis. MDA-MB231-luc cells were injected into the tail vein of female nude mice and the mice were then treated with DMSO, YF479 (20 mg/kg, 30 mg/kg) or SAHA (30 mg/kg). Due to size restrictions of murine capillaries, human tumor cells are rarely able to pass from the arterial to the venous system (or vice versa) by way of the lungs [43]. Therefore, shortly after tail vein injection, all detectable cells became trapped in the lung (Figure 5*A* day 0). Within the first few days, there was a substantial attenuation of bioluminescence signal in all groups (Figure 5*A* day 7). However, the presence of MDA-MB231-luc cells in the lungs of YF479-treated mice was much less than those in the control group after day 7 (Figure 5*B*). Previous study showed that the experimental metastasis model finely mimics both early stage (0–7 days) and late stage tumor metastasis. To evaluate the inhibitory effect of YF479 on tumor cell proliferation and apoptosis, we detected the expression of PCNA and cleaved-caspase 3 levels in lung sections. Our data indicated that YF479 inhibited tumor cell proliferation and induced tumor cell apoptosis in the lungs (Figure 5*C*). Therefore, these results demonstrated that YF479 inhibits breast tumor metastasis to the lungs.

YF479 Inhibits Cancer Metastasis to the Lungs at both Early and Late Stages

The early stages of tumor metastasis result in the formation of clinically occult micrometastatic foci and later stages primarily reflect the progressive, organ-destructive growth of already advanced metastases [44]. *In vitro* and *in vivo* experiments have shown that YF479 inhibited tumor growth and metastasis. Here, we used an animal model to investigate the effect of YF479 on early or late stages of metastatic progression. To target early or late-stage metastasis selectively, mice were administered with YF479 (30 mg/kg) either 0–7 or 7–15 d after intravenous injection of MDA-MB231-luc cells. Intriguingly, YF479 significantly ($P < .05$) hindered both early-stage and late-stage tumor metastases (Supplementary Figure S8). These results indicated that YF479 inhibits tumor cell metastasis at any stages.

YF479 Suppresses Local-regional Recurrence, Distant Metastasis and Prolongs Survival of Mice Orthotopically Implanted with 4 T1 Mammary Tumor Cells

The majority of invasive and noninvasive breast cancers are treated today by breast conservation therapy (BCT), which includes wide local excision and radiation treatment to the breast [45,46]. The incidence of local-regional recurrence (LRR) and distant metastases after BCT is positively correlated to the grade of malignancy [46]. Therefore, we hypothesized that YF479 adjuvant treatment would reduce LRR, inhibit distant metastasis formation, and prolong survival following surgical resection of the initial breast tumor. To test this hypothesis, we established the mouse 4 T1 mammary carcinoma model simulating an adjuvant treatment condition. 4 T1 growth characteristics parallel highly invasive human metastatic mammary carcinoma and the extent of disease is comparable with human stage IV breast cancer [47]. Tumor recurrence in mice was monitored using an in vivo bioluminescence imager (Figure 6*A*). The incidence of recurrence in the control, YF479 (20 mg/kg, 30 mg/kg) and SAHA (30 mg/kg) treatment groups were 90.91% (10 of 11), 54.54% (6 of 11), 27.27% (3 of 11), and 45.45% (5 of 11), respectively. Moreover, the respective incidences of distant metastasis in the control group, YF479 and SAHA treatment groups were 100% (11 of 11), 72.73% (8 of 11), 27.27% (3 of 11), and 54.54% (6 of 11) (Figure 6*B*). To detect whether the tumor suppression effect of YF479 treatment could yield a survival benefit, survival rate within the four groups was calculated. Our data showed that YF479 significantly increased the overall survival. By day 38, all the mice in control group had died, while only one mouse died in YF479 treatment group (30 mg/kg). On day 54, seven YF479-treated mice still lived (YF479 30 mg/kg) (Figure 6*C*). Altogether, YF479 suppressed local-regional recurrences and distant metastasis, and prolonged the survival of mice with breast cancer.

The Potential Toxicity Test of YF479 on Mice

The potential toxicity of YF479 (30 mg kg^{-1} day^{-1}) was detected by measuring changes in body weight and observing the renal function, hepatic function and other key organs by morphological analyses of major organs compared with control. Our results indicated no obvious architectural disarray following YF479 treatment (Supplementary Figure S9). It implies that YF479 has few side effects on the mouse body, at least under our therapeutic concentration.

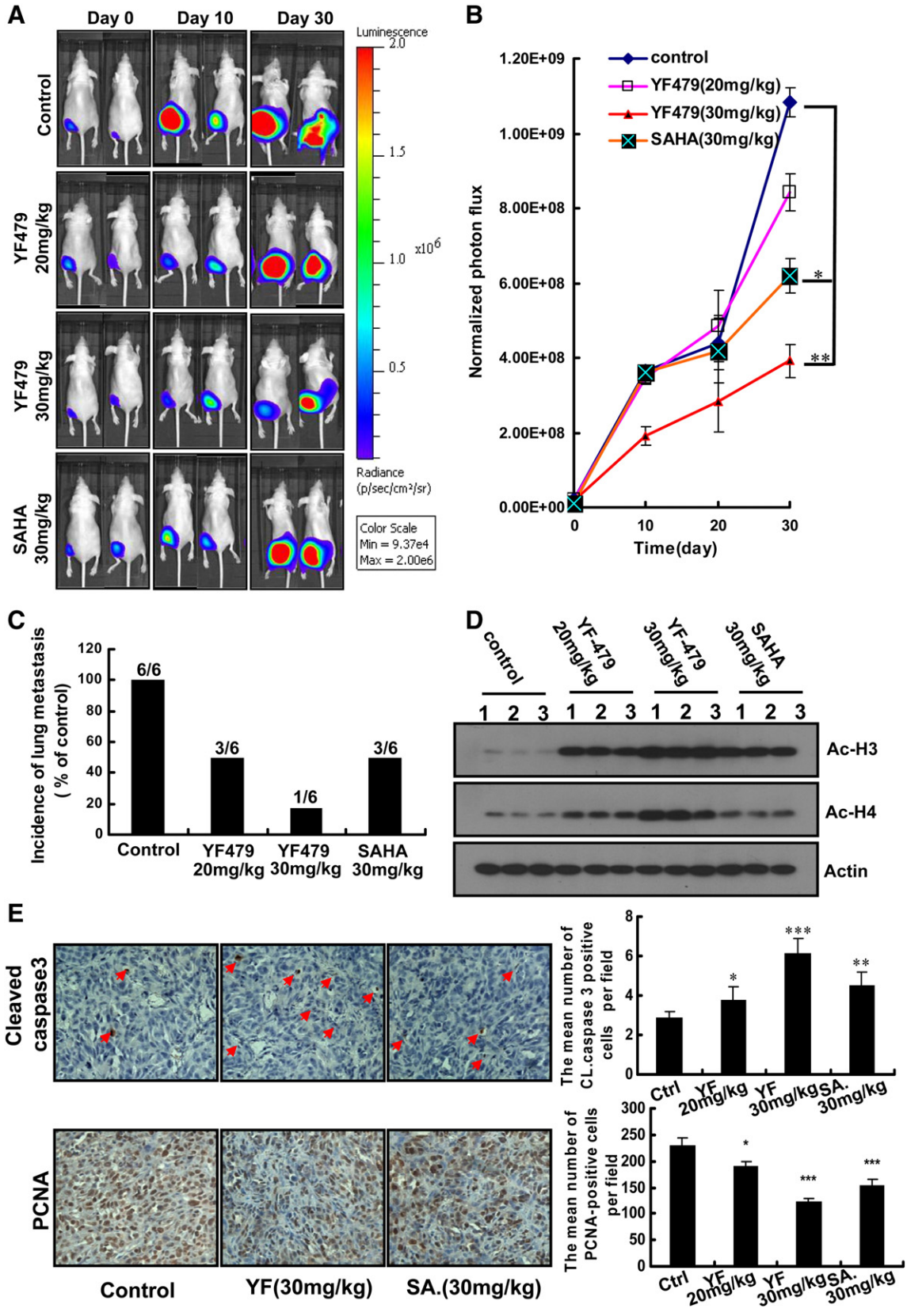

Figure 4. YF479 inhibits breast tumor growth and metastasis in mouse orthotopic implantation model. MDA-MB231-luc cells (1×10^6) were injected into mouse mammary fat pads. Mice were divided into 4 groups (n = 6 per group) based on the initial bioluminescence obtained on day 5 after tumor cell implantation. (A) Temporal in vivo bioluminescence images of mice bearing orthotropic (mammary fat pad)–injected MDA-MB231-luc cells. (B) Quantization of whole-body bioluminescence (total photon flux) in control and treatment groups. (C) Survey of metastasis site (lung) monitored by ex vivo bioluminescence detection of MDA-MB231-Luc cells in excised organ from control and treatment tumor-bearing nude mice. (D) YF479 upregulated the expression of Ac-H3, H4 in primary tumor. (E) Immunohistochemical analysis of primary tumor sections showed YF479 inhibited tumor cell proliferation (PCNA) and induced apoptosis (cleaved-caspase 3). *$P < .05$; **$P < .01$; ***$P < .001$ versus control.

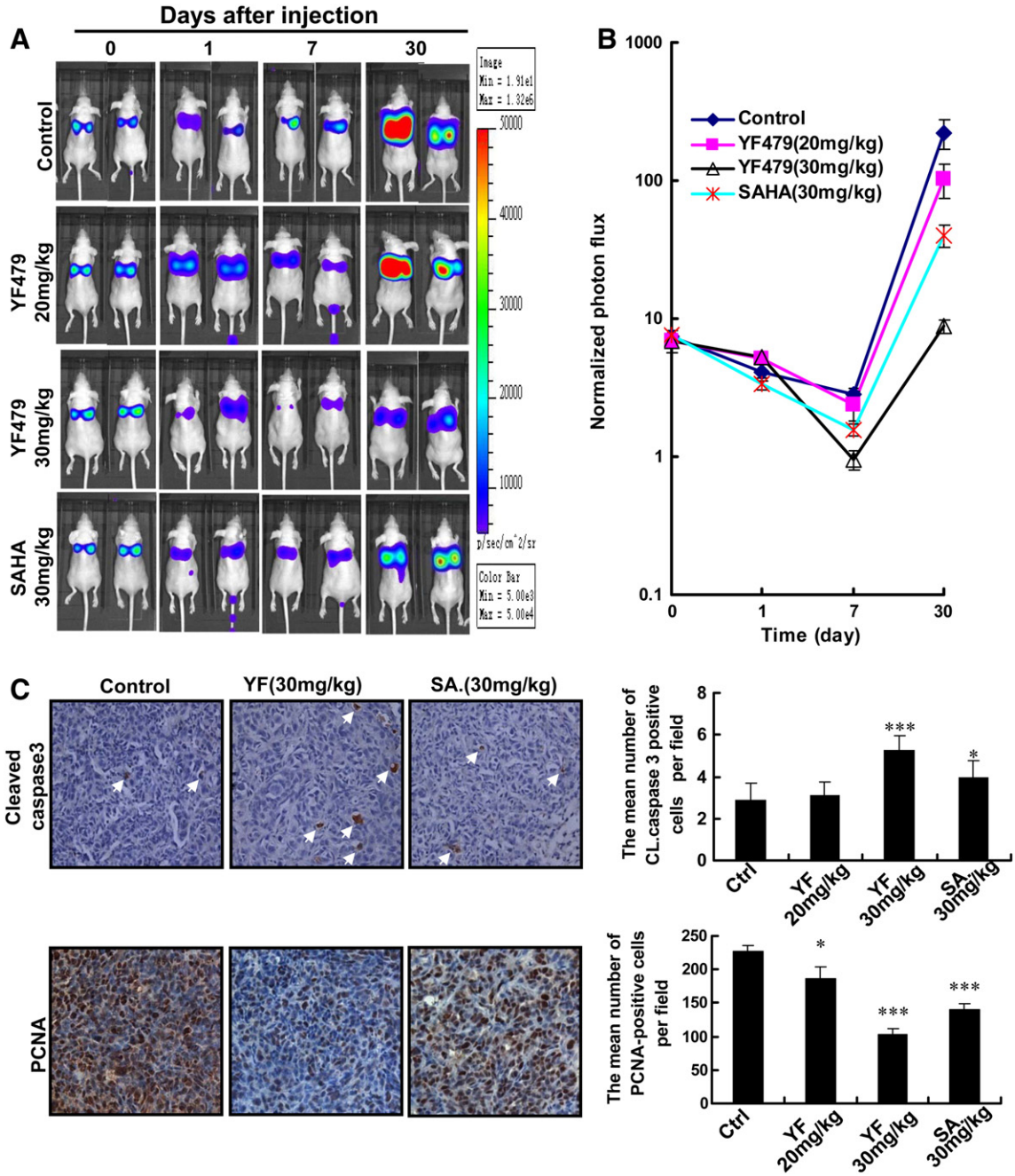

Figure 5. Effect of YF479 on blocking breast tumor metastases to the lung in an experimental animal model. After tail vein injection of MDA-MB231-luc cells (1×10^6), the mice were divided into four groups based on the initial bioluminescence images (n = 7 per group). Bioluminescence images were obtained using a Xenogen IVIS 2000 Biophotonic Imager at indicated times. (A) Representative bioluminescence images of mice inoculated with human MDA-MB231-luc cells in control and treatment groups. (B) Quantification of A. (C) YF479 upregulated cleaved-caspase 3 expression and suppressed the expression of PCNA. *$P < 0.05$; *** $P < .001$ versus control.

Discussion

In recent years, different classes of HDAC inhibitors have been in clinical investigation for the treatment of both hematologic and solid tumors. Importantly, except for their antitumor activity, data from clinical trials showed that HDAC inhibitors are well tolerated and possess limited toxicities that are rapidly reversible upon discontinuation of the drug [14,48]. In this study, we identified a novel hydroxamic acid-based HDACI, YF479. Our study showed that YF479 exhibited potent breast tumor therapeutic efficacy *in vitro* and *in vivo*.

One of the important findings in this study is that YF479 displayed satisfactory therapeutic effect in an adjuvant chemotherapy animal model. The majority of breast cancers are treated by breast conservation therapy (BCT), which includes wide local excision and radiation treatment. A large percentage of breast cancers have already metastasized before the removal of the localized primary tumor. These metastases are always hard to detect, but once they progress, they can lead to death. Adjuvant therapy of cancer following primary resection is often used in an attempt to eradicate metastases, and can lead to improved outcomes for patients [49]. Therefore,

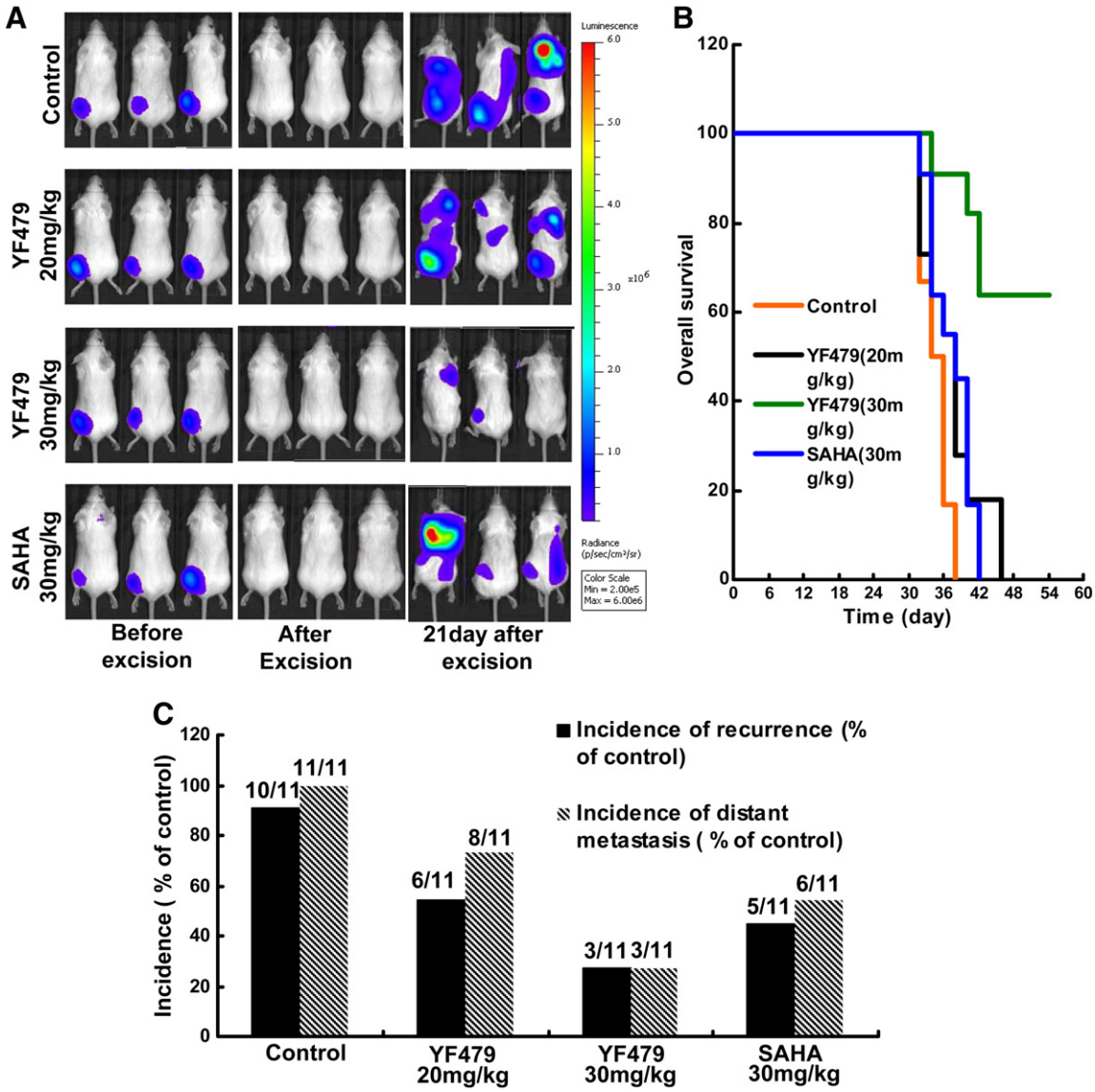

Figure 6. YF479 suppresses local-regional recurrence and distant metastasis, and increases survival of mice with breast cancer. 4 T1-luc cells (1×10^5) were injected into BALB/c mouse mammary fat pads. Primary mammary tumors were surgically removed 8 days after inoculation, and mice were treated with DMSO, YF479 (30 mg/kg) or SAHA (30 mg/kg) (n = 11 per group). (A) Representative bioluminescent images of mice in different groups. (B) Incidence of LRR and distant metastasis in each group. (C) Overall survival rate according to treatment in the adjuvant treatment model was shown. Time scale relates to days after tumor resection.

selection of the proper adjuvant therapy agent is very important for patients undergoing BCT. In our adjuvant therapy model, YF479 significantly reduced the incidence of LRR and distant metastasis. More important, tumor-bearing mice treated with YF479 demonstrated a tendency toward increased survival compared to control mice (Figure 6). The most common type of LRR, present in 57% to 88% of patients, appears at the site of the primary breast cancer and probably represents incomplete resection of the initial carcinoma. Although we did not detect any tumor cells after primary tumor resection by IVIS, it is possible that a few cells remained. This may partially explain the phenomenon that the vast majority of recurrence appears at the primary breast cancer site in mice. The inhibitory efficacy of YF479 in LRR stemming from primary tumor incomplete resection is likely due to its anti-tumor growth efficacy. Another possible reason for local-regional recurrence or distant metastatic growth in the lungs is the presence of disseminated tumor cells or circulating tumor cells [50]. We speculated that YF479 suppressed local recurrence or distant metastases via affecting disseminated tumor cell or circulating tumor cell survival. These results also implied that HDACs may play a critical role in tumor recurrence and distant metastasis. In aggregate, our data showed that YF479 provides significant clinical benefits in the treatment of breast cancer.

We have shown in this study that YF479 inhibited tumor growth and metastasis using orthotopic implantation and experimental animal models. Although clinical data showed that HDACIs have only moderate effects on solid tumor growth, we still obtained significant suppression of breast tumor growth by YF479. Interestingly, YF479 has a stronger anti-tumor growth activity compared with SAHA. We also believe that YF479 in combination with other anti-tumor agents is a reasonable therapeutic strategy for breast cancer progression. Metastasis is a complex process and one of the critical steps during tumor metastasis is tumor cell migration and invasion,

which are responsible for tumor cell entry into the lymphatic vessels or the bloodstream as well as their extravasation into the target organs [51]. Moreover, tumor metastasis still represents the major cause of mortality, being responsible for 90% of all cancer deaths. Indeed, in xenograft mouse models (Figures 4 and 5), metastasis (lung) was found to be blocked in mice with YF479 treatment. Furthermore, histological analysis demonstrated that YF479 induced tumor cell proliferation arrest and apoptosis in secondary tumors. This data implied that YF479 inhibited tumor metastasis partly via impeding tumor growth in target organs (such as lungs).

Previous investigations indicated that the early stages of tumor metastasis result in the formation of micro-metastatic foci and advanced stages primarily reflect the progressive, organ-destructive growth of already established metastases [26]. Although the medical conditions and means of diagnosis have greatly improved, patients who die from cancer succumb to treatment-refractory metastatic progression. These results may be caused by the limited function of some clinical and preclinical drugs. For example, matrix metalloproteinase (MMP) inhibitors and the fascin inhibitor Macroketone are only believed to impair initial metastasis events (early stage) [52,53]. Actually, effective anti-metastatic therapeutic drugs, such as dasatinib, medroxyprogesterone acetate and LY2157299 (TGF-βR I kinase inhibitor) [44], must be capable of impairing the proliferation and survival of already disseminated carcinoma cells. Here, we demonstrated that YF479 suppressed both early stage and advanced stage tumor metastasis (Supplementary Figure S8). These results suggested that YF479 displays potential therapeutic effects in clinical experiments.

Based on our studies, YF479 could be as a potential chemotherapy agent for breast cancer growth, metastasis and recurrence. In *in vitro* assays, while YF479 and SAHA both exhibited anti-breast tumor cell growth and motility efficacy, YF479 displayed significantly higher activity. Furthermore, YF479 abrogated cell growth, induced significant G2/M cell cycle arrest, and enhanced apoptosis in both human and mouse breast cancer cells. In addition, HDACIs also have beneficial clinical therapeutic effects on several types of cancer (lung, colorectal, sarcoma, etc.), and it will be essential to determine the efficacy of YF479 against other cancer types. Future studies may expand its role in combination with chemotherapy for breast cancer and a broader spectrum of other tumors.

Supplementary data to this article can be found online at http://dx.doi.org/10.1016/j.neo.2014.07.009.

Acknowledgments

We thank Dr. Stefan Siwko at Texas A&M University Health Science Center for his comments and editing.

Conflict of interest statement: none declared.

References

[1] Hanahan D and Weinberg RA (2000). The hallmarks of cancer. *Cell* **100**, 57–70.

[2] Bolden JE, Peart MJ, and Johnstone RW (2006). Anticancer activities of histone deacetylase inhibitors. *Nat Rev Drug Discov* **5**, 769–784.

[3] Khan O and Thangue La (2011). NB HDAC inhibitors in cancer biology: emerging mechanisms and clinical applications. *Immunol Cell Biol* **90**, 85–94.

[4] Marks P, Rifkind RA, Richon VM, Breslow R, Miller T, and Kelly WK (2001). Histone deacetylases and cancer: causes and therapies. *Nat Rev Cancer* **1**, 194–202.

[5] Jacobson S and Pillus L (1999). Modifying chromatin and concepts of cancer. *Curr Opin Genet Dev* **9**, 175–184.

[6] Johnstone RW (2002). Histone-deacetylase inhibitors: novel drugs for the treatment of cancer. *Nat Rev Drug Discov* **1**, 287–299.

[7] Catley L, Weisberg E, Tai YT, Atadja P, Remiszewski S, Hideshima T, Mitsiades N, Shringarpure R, LeBlanc R, and Chauhan D, et al (2003). NVP-LAQ824 is a potent novel histone deacetylase inhibitor with significant activity against multiple myeloma. *Blood* **102**, 2615–2622.

[8] Mann BS, Johnson JR, Cohen MH, Justice R, and Pazdur R (2007). FDA approval summary: vorinostat for treatment of advanced primary cutaneous T-cell lymphoma. *Oncologist* **12**, 1247–1252.

[9] Gryder BE, Sodji QH, and Oyelere AK (2012). Targeted cancer therapy: giving histone deacetylase inhibitors all they need to succeed. *Future Med Chem* **4**, 505–524.

[10] Tan J, Cang S, Ma Y, Petrillo RL, and Liu D (2010). Novel histone deacetylase inhibitors in clinical trials as anti-cancer agents. *J Hematol Oncol* **3**, 5–17.

[11] Jemal A, Center MM, DeSantis C, and Ward EM (2010). Global patterns of cancer incidence and mortality rates and trends. *Cancer Epidemiol Biomarkers Prev* **19**, 1893–1907.

[12] Munster PN, Marchion D, Thomas S, Egorin M, Minton S, Springett G, Lee JH, Simon G, Chiappori A, and Sullivan D, et al (2009). Phase I trial of vorinostat and doxorubicin in solid tumours: histone deacetylase 2 expression as a predictive marker. *Br J Cancer* **101**, 1044–1050.

[13] de la Vega M, Diaz-Canton E, and Alvarez RH (2012). Novel targeted agents for the treatment of advanced breast cancer. *Future Med Chem* **4**, 893–914.

[14] Luu TH, Morgan RJ, Leong L, Lim D, McNamara M, Portnow J, Frankel P, Smith DD, Doroshow JH, and Wong C, et al (2008). A phase II trial of vorinostat (suberoylanilide hydroxamic acid) in metastatic breast cancer: a California Cancer Consortium study. *Clin Cancer Res* **14**, 7138–7142.

[15] Munster PN, Thurn KT, Thomas S, Raha P, Lacevic M, Miller A, Melisko M, Ismail-Khan R, Rugo H, and Moasser M, et al (2011). A phase II study of the histone deacetylase inhibitor vorinostat combined with tamoxifen for the treatment of patients with hormone therapy-resistant breast cancer. *Br J Cancer* **104**, 1828–1835.

[16] Zhang T, Li J, Dong Y, Zhai D, Lai L, Dai F, Deng H, Chen Y, Liu M, and Yi Z (2012). Cucurbitacin E inhibits breast tumor metastasis by suppressing cell migration and invasion. *Breast Cancer Res Treat* **135**, 445–458.

[17] Fang Y, Chen Y, Yu L, Zheng C, Qi Y, Li Z, Yang Z, Zhang Y, Shi T, and Luo J, et al (2013). Inhibition of breast cancer metastases by a novel inhibitor of TGFbeta receptor 1. *J Natl Cancer Inst* **105**, 47–58.

[18] Gediya LK, Chopra P, Purushottamachar P, Maheshwari N, and Njar VC (2005). A new simple and high-yield synthesis of suberoylanilide hydroxamic acid and its inhibitory effect alone or in combination with retinoids on proliferation of human prostate cancer cells. *J Med Chem* **48**, 5047–5051.

[19] Baschnagel A, Russo A, Burgan WE, Carter D, Beam K, Palmieri D, Steeg PS, Tofilon P, and Camphausen K (2009). Vorinostat enhances the radiosensitivity of a breast cancer brain metastatic cell line grown in vitro and as intracranial xenografts. *Mol Cancer Ther* **8**, 1589–1595.

[20] Dong Y, Lu B, Zhang X, Zhang J, Lai L, Li D, Wu Y, Song Y, Luo J, and Pang X, et al (2010). Cucurbitacin E, a tetracyclic triterpenes compound from Chinese medicine, inhibits tumor angiogenesis through VEGFR2-mediated Jak2-STAT3 signaling pathway. *Carcinogenesis* **31**, 2097–2104.

[21] Lopez G, Liu J, Ren W, Wei W, Wang S, Lahat G, Zhu QS, Bornmann WG, McConkey DJ, and Pollock RE, et al (2009). Combining PCI-24781, a novel histone deacetylase inhibitor, with chemotherapy for the treatment of soft tissue sarcoma. *Clin Cancer Res* **15**, 3472–3483.

[22] Khare V, Lyakhovich A, Dammann K, Lang M, Borgmann M, Tichy B, Pospisilova S, Luciani G, Campregher C, and Evstatiev R, et al (2012). Mesalamine modulates intercellular adhesion through inhibition of p-21 activated kinase-1. *Biochem Pharmacol* **85**, 234–244.

[23] Song Y, Dai F, Zhai D, Dong Y, Zhang J, Lu B, Luo J, Liu M, and Yi Z (2012). Usnic acid inhibits breast tumor angiogenesis and growth by suppressing VEGFR2-mediated AKT and ERK1/2 signaling pathways. *Angiogenesis* **15**, 421–432.

[24] Gumireddy K, Li A, Gimotty PA, Klein-Szanto AJ, Showe LC, Katsaros D, Coukos G, Zhang L, and Huang Q (2009). KLF17 is a negative regulator of epithelial-mesenchymal transition and metastasis in breast cancer. *Nat Cell Biol* **11**, 1297–1304.

[25] Pan X, Han H, Wang L, Yang L, Li R, Li Z, Liu J, Zhao Q, Qian M, and Liu M, et al (2011). Nitidine chloride inhibits breast cancer cells migration and invasion by suppressing c-Src/FAK associated signaling pathway. *Cancer Lett* **313**, 181–191.

[26] DeLisser H, Liu Y, Desprez PY, Thor A, Briasouli P, Handumrongkul C, Wilfong J, Yount G, Nosrati M, and Fong S, et al (2010). Vascular endothelial platelet endothelial cell adhesion molecule 1 (PECAM-1) regulates advanced metastatic progression. *Proc Natl Acad Sci U S A* **107**, 18616–18621.

[27] Kershaw MH, Jackson JT, Haynes NM, Teng MW, Moeller M, Hayakawa Y, Street SE, Cameron R, Tanner JE, and Trapani JA, et al (2004). Gene-engineered T cells as a superior adjuvant therapy for metastatic cancer. *J Immunol* **173**, 2143–2150.

[28] Somech R, Izraeli S, and A JS (2004). Histone deacetylase inhibitors – a new tool to treat cancer. *Cancer Treat Rev* **30**, 461–472.

[29] Hanahan D and Weinberg RA (2011). Hallmarks of cancer: the next generation. *Cell* **144**, 646–674.

[30] Yan L, Donze JR, and Liu L (2005). Inactivated MGMT by O6-benzylguanine is associated with prolonged G2/M arrest in cancer cells treated with BCNU. *Oncogene* **24**, 2175–2183.

[31] Yang F, von Knethen A, and Brune B (2000). Modulation of nitric oxide-evoked apoptosis by the p53-downstream target p21(WAF1/CIP1). *J Leukoc Biol* **68**, 916–922.

[32] Zhao H, Ho PC, Lo YH, Espejo A, Bedford MT, Hung MC, and Wang SC (2012). Interaction of proliferation cell nuclear antigen (PCNA) with c-Abl in cell proliferation and response to DNA damages in breast cancer. *PLoS One* **7**, e29416.

[33] Yang CJ, Wang CS, Hung JY, Huang HW, Chia YC, Wang PH, Weng CF, and Huang MS (2009). Pyrogallol induces G2-M arrest in human lung cancer cells and inhibits tumor growth in an animal model. *Lung Cancer* **66**, 162–168.

[34] Han J, Kim S, Yang JH, Nam SJ, and Lee JE (2012). TPA-induced p21 expression augments G2/M arrest through a p53-independent mechanism in human breast cancer cells. *Oncol Rep* **27**, 517–522.

[35] Brauns SC, Dealtry G, Milne P, Naude R, and Van de Venter M (2012). Caspase-3 activation and induction of PARP cleavage by cyclic dipeptide cyclo (Phe-Pro) in HT-29 cells. *Anticancer Res* **72**, 4130–4140.

[36] Chen J and Gallo KA (2012). MLK3 regulates paxillin phosphorylation in chemokine-mediated breast cancer cell migration and invasion to drive metastasis. *Cancer Res* **25**, 4197–4202.

[37] Chen LC, Tu SH, Huang CS, Chen CS, Ho CT, Lin HW, Lee CH, Chang HW, Chang CH, and Wu CH, et al (2012). Human breast cancer cell metastasis is attenuated by lysyl oxidase inhibitors through down-regulation of focal adhesion kinase and the paxillin-signaling pathway. *Breast Cancer Res Treat* **134**, 989–1004.

[38] Deakin NO and Turner CE (2011). Distinct roles for paxillin and Hic-5 in regulating breast cancer cell morphology, invasion, and metastasis. *Mol Biol Cell* **22**, 327–341.

[39] Chen Q, Hongu T, Sato T, Zhang Y, Ali W, Cavallo JA, van der Velden A, Tian H, Di Paolo G, and Nieswandt B, et al (2012). Key roles for the lipid signaling enzyme phospholipase d1 in the tumor microenvironment during tumor angiogenesis and metastasis. *Sci Signal* **5**, ra79.

[40] Yuan K, Frolova N, Xie Y, Wang D, Cook L, Kwon YJ, Steg AD, Serra R, and Frost AR (2010). Primary cilia are decreased in breast cancer: analysis of a collection of human breast cancer cell lines and tissues. *J Histochem Cytochem* **58**, 857–870.

[41] Deryugina EI and Quigley JP (2006). Matrix metalloproteinases and tumor metastasis. *Cancer Metastasis Rev* **25**, 9–34.

[42] An Z, Gluck CB, Choy ML, and Kaufman LJ (2010). Suberoylanilide hydroxamic acid limits migration and invasion of glioma cells in two and three dimensional culture. *Cancer Lett* **292**, 215–227.

[43] Minn AJ, Kang Y, Serganova I, Gupta GP, Giri DD, Doubrovin M, Ponomarev V, Gerald WL, Blasberg R, and Massague J (2005). Distinct organ-specific metastatic potential of individual breast cancer cells and primary tumors. *J Clin Invest* **115**, 44–55.

[44] Valastyan S and Weinberg RA (2011). Tumor metastasis: molecular insights and evolving paradigms. *Cell* **147**, 275–292.

[45] Ponzone R and Baum M (2012). Loco-regional therapy and breast cancer survival: Searching for a link. *Breast* **22**, 510–514.

[46] Huston TL and Simmons RM (2005). Locally recurrent breast cancer after conservation therapy. *Am J Surg* **189**, 229–235.

[47] Pulaski BA, Terman DS, Khan S, Muller E, and Ostrand-Rosenberg S (2000). Cooperativity of Staphylococcal aureus enterotoxin B superantigen, major histocompatibility complex class II, and CD80 for immunotherapy of advanced spontaneous metastases in a clinically relevant postoperative mouse breast cancer model. *Cancer Res* **60**, 2710–2715.

[48] Kelly WK, O'Connor OA, Krug LM, Chiao JH, Heaney M, Curley T, MacGregore-Cortelli B, Tong W, Secrist JP, and Schwartz L, et al (2005). Phase I study of an oral histone deacetylase inhibitor, suberoylanilide hydroxamic acid, in patients with advanced cancer. *J Clin Oncol* **23**, 3923–3931.

[49] Bergh J, Jonsson PE, Glimelius B, and Nygren P (2001). A systematic overview of chemotherapy effects in breast cancer. *Acta Oncol* **40**, 253–281.

[50] Bidard FC, Vincent-Salomon A, Gomme S, Nos C, de Rycke Y, Thiery JP, Sigal-Zafrani B, Mignot L, Sastre-Garau X, and Pierga JY (2008). Disseminated tumor cells of breast cancer patients: a strong prognostic factor for distant and local relapse. *Clin Cancer Res* **14**, 3306–3311.

[51] Steeg PS (2006). Tumor metastasis: mechanistic insights and clinical challenges. *Nat Med* **12**, 895–904.

[52] Kessenbrock K, Plaks V, and Werb Z (2010). Matrix metalloproteinases: regulators of the tumor microenvironment. *Cell* **141**, 52–67.

[53] Chen L, Yang S, Jakoncic J, Zhang JJ, and Huang XY (2010). Migrastatin analogues target fascin to block tumour metastasis. *Nature* **464**, 1062–1066.